

Numerical Studies of Adaptive Finite Element Methods for Two Dimensional Convection-Dominated Problems

Pengtao Sun · Long Chen · Jinchao Xu

Received: 17 April 2009 / Revised: 10 September 2009 / Accepted: 10 November 2009 /
Published online: 20 November 2009
© Springer Science+Business Media, LLC 2009

Abstract In this paper, we study the stability and accuracy of adaptive finite element methods for the convection-dominated convection-diffusion-reaction problem in the two-dimension space. Through various numerical examples on a type of layer-adapted grids (Shishkin grids), we show that the mesh adaptivity driven by accuracy alone cannot stabilize the scheme in all cases. Furthermore the numerical approximation is sensitive to the symmetry of the grid in the region where the solution is smooth. On the basis of these two observations, we develop a multilevel-homotopic-adaptive finite element method (MHAFEM) by combining streamline diffusion finite element method, anisotropic mesh adaptation, and the homotopy of the diffusion coefficient. We use numerical experiments to demonstrate that MHAFEM can efficiently capture boundary or interior layers and produce accurate solutions.

Keywords Convection-dominated convection-diffusion-reaction problem · Layer-adapted Shishkin grids · Streamline diffusion finite element · Anisotropic adaptive mesh · Multilevel homotopic adaptive finite element method

P. Sun (✉)
Department of Mathematical Sciences, University of Nevada, Las Vegas, 4505 Maryland Parkway,
Las Vegas, NV 89154, USA
e-mail: pengtao.sun@unlv.edu

L. Chen
Department of Mathematics, University of California, Irvine, Irvine, CA 92697, USA
e-mail: chenlong@math.uci.edu

J. Xu
Department of Mathematics, Pennsylvania State University, University Park, PA 16802, USA
e-mail: xu@math.psu.edu

1 Introduction

In this paper we shall study numerical approximations for the following convection-dominated convection-diffusion-reaction equation

$$-\varepsilon \Delta u + \mathbf{b} \cdot \nabla u + cu = f, \quad (1)$$

posed in two dimensional polygonal domains Ω with appropriate boundary conditions. We are interested in the convection-dominated case, namely $\varepsilon \ll \|\mathbf{b}\|_\infty$, which may come from a linearized Navier-Stokes equation with high Reynolds number, the drift-diffusion equations of semiconductor device modeling, and the Black-Scholes equation from financial modeling. We shall report our discovery on the stabilization and accuracy of the adaptive finite element methods and develop a new method to attack this difficult problem.

Due to the small diffusion, the solution to (1) has singularities in the form of boundary or interior layers. The standard numerical approximation, e.g., standard finite element method, on quasi-uniform grids will yield nonphysical oscillations unless the mesh is fine enough to capture the layers [37, 38, 40]. As pointed out in the book by Morton [38], “*Accurate modeling of the interaction between convective and diffusive processes is the most ubiquitous and challenging task in the numerical approximation of partial differential equations.*”

To obtain a robust numerical approximation for convection-dominated problems, one approach is to modify the discretization of the convection term while keeping the underlying uniform or quasi-uniform grids unchanged. Techniques developed along this line include upwind scheme [18], streamline diffusion finite element method (SDFEM), also known as streamline-upwind/Petrov-Galerkin formulation (SUPG) [12, 24], residual free bubbles (RFB) functions [7–10], exponential fitting [1, 11, 39, 46], discontinuous Galerkin methods [6, 21], and spurious oscillations at layers diminishing (SOLD) methods [26, 27]. Note that this list is by no means exhaustive; there are many other stabilization techniques.

Another approach is to adapt the underlying grids to capture the layers while keeping the standard or simple schemes. The effect of the mesh adaptation for convection-dominated problem is twofold: stability and accuracy. Usually these two issues are coupled together. In practice, researchers observe that once the accuracy is improved through the mesh adaption, so is the stability, cf., [5, 34, 47]. One folklore in this approach is that if the grids are “correctly” adapted to the layers, the standard finite element method will be stable and produce almost optimal rate of convergence; see some numerical evidences in [30, 34, 47] and some theoretical justification for a model problem in [35, 48]. Here “correctly” adaptive grids are meant to adaptive grids based on which the finite element space can provide the optimal or quasi-optimal approximation property.

In our recent work [17], we provide a mathematical proof on the accuracy and stability of the mesh adaptation for a 1-d singularly perturbed problem. We found that even the underlying grid can provide accurate approximation, the numerical scheme could be still unstable. Moreover the accuracy depends crucially on the uniformity of the grids which are away from the singularity.

In this paper, we shall extend our studying to 2-d by carrying out various numerical examples on a type of lay-adapted grids. We shall provide numerical evidences to support the insight we proved for 1-d problems. Here we want to highlight one example which only presents parabolic layers. We use correctly layer-adapted grids, so-called Shishkin grids, such that the finite element space based on such grids can provide quasi-optimal approximation. A common believe of the community of Shishkin type grids [31, 33–37, 41–43, 45, 48] is that once the layer is fully resolved (enough mesh points inside the layer) then the scheme is stabilized and further holds the optimal or quasi-optimal convergence rate.

We shall numerically show this is not always true. More precisely, we use the standard finite element method combining with a specific layer-adapted grid to solve problems (1) that presents parabolic boundary layers only. The finite element space based on the layer-adapted grids can provide the exactly optimal approximation. However the numerical approximation is unstable when the number of grid points in the convection direction is odd and the grid size is quasi-uniform. Moreover, such unstable standard scheme can be stabilized by having even number of grid points or having a grid size being ε along the convection direction. We will show these phenomena by doing several numerical examples in this paper.

On the other hand, even the standard finite element method is stable in some cases, we further show that the accuracy depends crucially on the uniformity of the grids which are away from the singularity. The accuracy of the approximation is very sensitive to the perturbation of grid points in the region where the solution is smooth but, in contrast, it is robust with respect to the perturbation of properly adapted grid points inside the boundary or interior layers. When the grid is only quasi-uniform in the smooth part, in general, we can only expect a first order convergence rate instead of second order in L_∞ and L_2 norm when piecewise linear finite element is used.

From these numerical examples, we conclude that the stabilization of schemes for convection-dominated problems is necessary even on layer-adapted grids. Among various stabilization techniques, we shall choose the streamline diffusion finite element method (SD-FEM) and demonstrate that SDFEM on correctly adapted grids gives stable and accurate approximation.

The next question is then how to construct such a correctly adapted grid. The layer-adapted grids using a priori information on the location of layers are not satisfactory in practice. It would be more desirable to construct such grids in a posteriori manner, namely by extracting information from numerical solutions. However, the study of the Shishkin type grids paves the way of understanding more complicated grid structures and has its theoretical value. This study would provide insight for some practically more meaningful cases, which are very hard to analyze theoretically.

Most a posteriori estimators constructed for elliptic type equations do not work well for the convection dominated problems. In [25], John presents a thoroughly numerical comparison of some standard a posteriori error estimators for convection-dominated equations, including residual-based error estimator, Zienkiewicz-Zhu estimator and error estimator based on the solution of local Neumann problems. He shows that no error estimator worked satisfactorily for all numerical examples. One reason is that the standard a posteriori error estimator for convection-dominated equations contains $1/\varepsilon$, cf. [28]. When ε is small, the resulting adaptive mesh refinement may put the refined mesh in a wrong place.

We shall solve this difficulty by the homotopy of the diffusion constant ε . By the theory of asymptotic expansion [20, 40], we know the solution of (1) depends continuously on ε . We start our computation for a large ε , say $\varepsilon = 1$, and apply adaptive mesh refinement to correctly adapt the mesh for this diffusion dominated elliptic problem. Then we decrease the value of ε by half, for example, and continue the mesh adaptation for the reduced ε . We continue in this way until the desired small value of ε is reached. We call such method as multilevel-homotopic-adaptive finite element method (MHAFEM).

Since the singularity occurring in convection-dominated problems (1) mostly presents in the type of layer, i.e., the directional derivative is large only in one direction. It is then natural to use anisotropic meshes which are stretched according to the anisotropy of the solution. We shall apply the anisotropic mesh adaptation developed in [14, 16, 44] to resolve such anisotropic singularity. We provide numerical examples, including Hemker problem [19], to show that our MHAFEM based on anisotropic mesh adaptation can capture the boundary layers and produce good numerical approximations.

To do so, we need an approximation of the Hessian matrix $\nabla^2 u$ using the numerical solution u_h . It could be done by firstly recover a continuous approximation of ∇u from discontinuous piecewise constant function ∇u_h and then take derivative to obtain a piecewise constant approximation of $\nabla^2 u$. There are several ways to recover a continuous approximation of ∇u . We shall use the approach proposed in [3, 4]. Namely first compute the L^2 projection of ∇u_h into the finite element space and then apply several multigrid smoothing. Mathematical proof of this approach under mild assumptions for isotropic mesh can be found at [3, 4]. Since the accuracy is sensitive to the mesh in the smooth region, local mesh smoothing developed in [13] is further applied to improve the symmetry of the mesh.

The rest of the paper is organized as follows. In Sect. 2, we provide several numerical examples to show the correct mesh adaptation can stabilize the standard finite element method and the symmetry of the mesh affects the convergence rate for the convection-dominated problem (1). Streamline diffusion finite element method (SDFEM) is introduced in Sect. 3, where we show that SDFEM can recover the stability and the accuracy of numerical solution via some examples with unstable solutions. In Sect. 4, we describe in detail our new method MHAFEM with anisotropic mesh adaptation, and illustrate its procedure and capacity by applying MHAFEM and SDFEM to a mathematical example with analytic solution and Hemker problem, respectively, where the first one possesses regular boundary layers and the second one bears sharp interior layers.

2 Stability and Accuracy of Standard Finite Element Methods

In this section, we shall investigate the stability and accuracy of the standard finite element methods on adaptive grids. We show two observations for convection-dominated problems. Firstly, even though the grids are adapted to the boundary or interior layers such that the corresponding finite element spaces provide good approximation property, the standard finite element methods could be still unstable. The second one is that the symmetry of the grid in the region where the solution is smooth is essential to obtain the optimal convergence rate.

We shall illustrate these numerical phenomena by considering the following boundary value problem

$$\begin{cases} -\varepsilon \Delta u + \mathbf{b} \cdot \nabla u + cu = f & \Omega \\ u = g & \partial\Omega \end{cases} \tag{2}$$

in the unit square domain $\Omega = (0, 1)^2$. The constant ε is positive. The coefficient functions b, c , the source data f , and the boundary data g are assumed to be sufficiently smooth.

The solution of (2) could have two types of boundary layers. One is called regular boundary layer which has width $O(\varepsilon)$. Another is called parabolic layer which has width $O(\sqrt{\varepsilon})$. We refer to [43] for details about these two types of boundary layers.

We denote by $L^2(\Omega)$ and $H^k(\Omega)$, $k \geq 1$, the standard Lebesgue and Sobolev spaces equipped with the norms $\|\cdot\|_0 = \|\cdot\|_{L^2(\Omega)}$, $\|\cdot\|_k = \|\cdot\|_{H^k(\Omega)}$. Let $H_g^1(\Omega) = \{v \in H^1(\Omega), v|_{\partial\Omega} = g\}$ and $H_0^1(\Omega) = \{v \in H^1(\Omega), v|_{\partial\Omega} = 0\}$. The weak formulation of (2) is to find $u \in H_g^1(\Omega)$ such that

$$a(u, v) = f(v), \quad \forall v \in H_0^1(\Omega), \tag{3}$$

where

$$a(u, v) := \varepsilon \int_{\Omega} \nabla u \cdot \nabla v \, dx + \int_{\Omega} (\mathbf{b} \cdot \nabla u + cu)v \, dx,$$

and for $f \in L^2(\Omega)$

$$f(v) := (f, v) := \int_{\Omega} f v \, dx.$$

Given a triangulation \mathcal{T}_h of Ω , we denote the piecewise linear and continuous finite element space by V^h , i.e.,

$$V^h = \{v \in H^1(\Omega), v|_{\tau} \in \mathcal{P}_1(\tau), \forall \tau \in \mathcal{T}_h\},$$

where $\mathcal{P}_1(\tau)$ is linear polynomial space in one element τ . We then define $V_g^h := V^h \cap H_g^1(\Omega)$ and $V_0^h := V^h \cap H_0^1(\Omega)$. The standard finite element method discretization of (3) is to find $u_h \in V_g^h$ such that

$$a(u_h, v_h) = f(v_h), \quad \forall v_h \in V_0^h. \tag{4}$$

The conventional subscript h is used to denote the mesh size, i.e., $h = \max_{\tau \in \mathcal{T}_h} \text{diam}(\tau)$ for shape regular triangulations. In the classical error estimate of finite element method, the mesh size h is used to measure the convergence rate over a sequence of quasi-uniform meshes. Since h does not make sense for adaptive grids, instead, we shall use N , the number of degree of freedom to measure the convergence rate. It is well known that for a uniform mesh in the two-dimension space, $h^2 = CN^{-1}$ and

$$\|u - u_I\|_0 \leq CN^{-1} \|u\|_2, \quad \text{for } u \in H^2(\Omega), \tag{5}$$

where u_I is the nodal interpolation of u . Similar second order interpolation error estimate holds in the L^∞ norm as well. Optimal error estimates for correctly adaptive meshes is obtained in [16, 23]. For this reason, we expect the optimal convergence rate of $\|u - u_h\|_0$ is second order.

Example 1: Approximations Based on Uniform Grids and Shishkin Grids for Solutions with Regular Boundary Layers

In this example, we show that for regular boundary layers, the layer-adapted grid will enhance the stability and accuracy of the standard finite element method. This is a well known result; see e.g. [35]. We include here for the purpose of completeness and comparison.

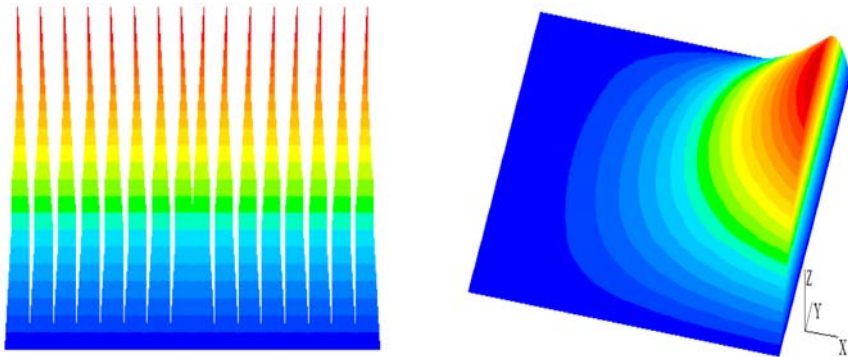
The example is given by $\varepsilon = 10^{-8}$, $\mathbf{b} = (1, 0)^T$, $c = 0$, and $g = 0$. The right hand side f and the boundary data g is chosen such that the solution of (2) is

$$u = (x^2 - e^{-\frac{1-x}{\varepsilon}})y(1 - y).$$

This function exhibits an exponential regular boundary layers near $\{x = 1\}$ which is perpendicular to the convection direction $(1, 0)^T$.

We first employ the standard finite element method (4) with bilinear element to solve (2) on uniform rectangular grids with $\varepsilon \ll h$. The numerical approximation presents oscillation, as displayed in Fig. 1(a).

Based on appropriate layer-adapted grids, standard finite element will produce stable and accurate numerical approximations. Figure 1(b) shows the numerical solution with standard piecewise bilinear element on a rectangular Shishkin grids [33, 37, 42, 43]. Briefly introducing, a Shishkin grid is a piecewise uniform grid with a mesh transition point. It is generated by a so-called mesh generating function $x = \phi(\xi)$ [33] which maps a uniform mesh in ξ onto a layer-adapted mesh in x . This mesh generating function $\phi(\xi)$ is related to a mesh



(a) An oscillating numerical approximation on a uniform mesh. The standard finite element method is used. (b) An accurate numerical approximation on a Shishkin mesh. The standard finite element method is used.

Fig. 1 (Color online) Example 1. Numerical approximations on different meshes for solutions with regular boundary layers. The standard finite element method is used

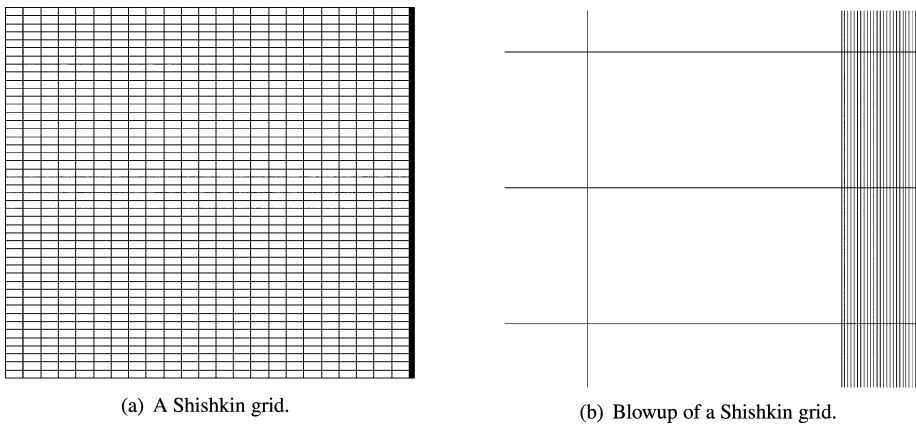


Fig. 2 Example 1. Shishkin grids for regular boundary layers

transition point λ that is given by the width of boundary layer. For this example, we uniformly generate $\frac{K}{2} \times K$ grids inside the boundary layer with the width $2\epsilon \ln(K)$ and outside of the layer, respectively. Figure 2 shows a Shishkin grid both globally and locally.

We list the convergence results in Tables 1 and 2 for the standard finite element approximation based on uniform and Shishkin grids, respectively. We use N to denote the number of unknowns, $e = \|u - u_h\|_\infty$ the approximation error in the L^∞ norm, and $|\frac{\ln e}{\ln N}|$ an estimate of the convergent rate. The second order convergence rate is then indicated by $|\frac{\ln e}{\ln N}| = 1$.

As shown in Fig. 1, the oscillating solution on uniform mesh derives unsatisfactory convergence rate, cf. Table 1, while almost the second order convergence rate is produced on Shishkin grids, cf., Table 2. Similar results also hold for Shishkin grids with odd number of unknowns in the convection direction.

Table 1 Example 1. Errors of standard FEM approximation on uniform grids for a solution with a regular boundary layer

N	$e = \ u - u_h\ _\infty$	$ \frac{\ln e}{\ln N} $
484	2.50E-01	0.2246
1024	2.50E-01	0.2001
2116	2.50E-01	0.1811
4096	2.50E-01	0.1667
8100	2.50E-01	0.1541
16384	2.50E-01	0.1429

Table 2 Example 1. Errors of standard FEM approximation on Shishkin grids for a solution with a regular boundary layer

N	$e = \ u - u_h\ _\infty$	$ \frac{\ln e}{\ln N} $
484	2.84E-03	0.9487
1024	9.79E-04	0.9996
2116	8.83E-04	0.9183
4096	3.55E-04	0.9551
8100	3.01E-04	0.9010
16384	1.29E-04	0.9230

Example 2: Approximations Based on Shishkin Grids for a Solution with Parabolic Layers

In this example, we show that for a solution with parabolic layers only, even though the grids are able to resolve the layer, the standard finite element method can still be unstable.

The example is given by $\varepsilon = 10^{-8}$, $\mathbf{b} = (1, 0)^T$, $c = 0$. The right hand side f and the boundary data g are chosen such that

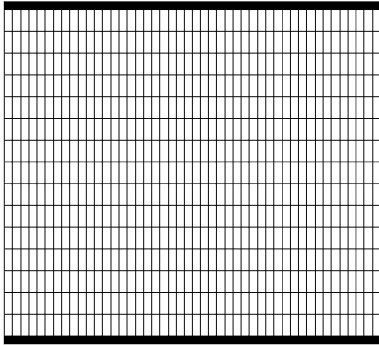
$$u = x^2(y(1 - y) + e^{-y/\sqrt{\varepsilon}} + e^{-(1-y)/\sqrt{\varepsilon}})$$

is the solution of (2); see Fig. 4(b). We choose the solution with parabolic boundary layers near $\{y = 0\}$ and $\{y = 1\}$, which are parallel to the convection direction $(1, 0)^T$.

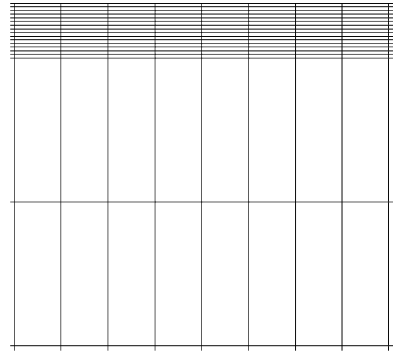
Shishkin grids for this problem are constructed as follows: we uniformly generate $\frac{K}{3} \times K$ grids inside the upper and lower parabolic boundary layers with the width $2\sqrt{\varepsilon} \ln(K)$, and outside of the layers, respectively. Figure 3(a) and 3(b) show such a Shishkin grid both globally and locally.

We first show the numerical result of Shishkin grid with odd number of unknowns in the convection direction $(1, 0)^T$. Figure 4(a) shows the oscillating numerical solution in this case. The corresponding unsatisfactory convergence rate is displayed in Table 3. However, as shown in Fig. 4(b) and Table 4, the smooth numerical solution and nearly optimal convergence rate are recovered by using even number of unknowns in the convection direction $(1, 0)^T$.

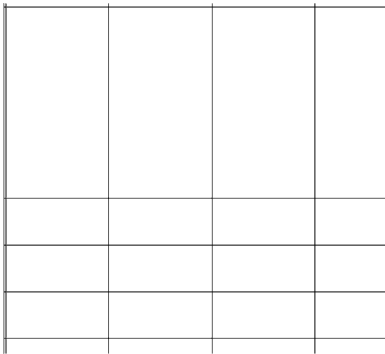
For the unstable case of Shishkin grid, i.e. odd number of unknowns in the convection direction $(1, 0)^T$, there is a simple way to recover the stability and eliminate the oscillation of the numerical solution. Counting from the left boundary, we move the second column of grid points to the left boundary such that the first grid size in the x -direction is ε , as shown in Fig. 3(c). Based on this grid, we are able to obtain nearly optimal accuracy; see Table 5. The location of such ε -width grid does not matter. For example, if we let the size of mid-grid at the center of smooth region in x -direction be ε (see Fig. 3(d)), then the nearly optimal convergence rate is recovered for a unstable Shishkin grids, as shown in Table 6, and the



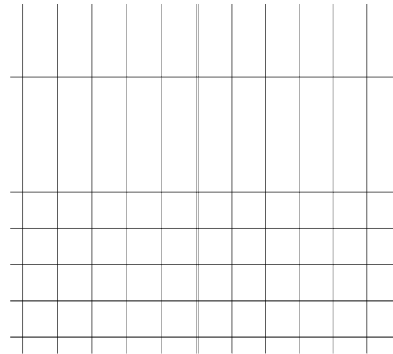
(a) A Shishkin grid for two parabolic boundary layers.



(b) Blowup of a Shishkin grid inside a parabolic boundary layer.

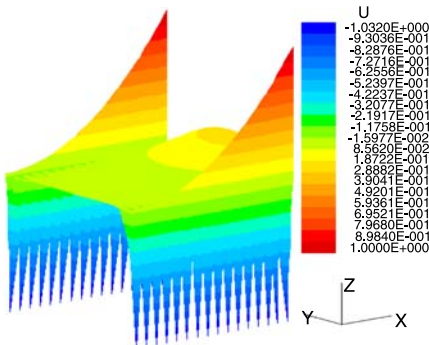


(c) A Shishkin grid with ϵ size for the first grid close to the left boundary in the x-direction.

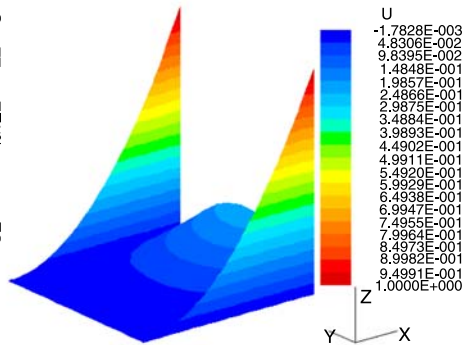


(d) A Shishkin grid with ϵ size for the mid-grid in the x-direction at the center of smooth region.

Fig. 3 Example 2. Shishkin grids for parabolic boundary layers



(a) An oscillating numerical approximation on a Shishkin mesh with odd number of unknowns in the convection direction.



(b) A smooth solution on a Shishkin mesh with even number of unknowns in the convection direction.

Fig. 4 (Color online) Example 2. Numerical approximations on different meshes for a solution with parabolic boundary layers

Table 3 Example 2. Errors of standard FEM approximations on Shishkin grids for a solution with parabolic layers: odd number of unknowns in the convection direction

N	$e = \ u - u_h\ _\infty$	$ \frac{\ln e}{\ln N} $
441	1.83E+01	0.4773
961	6.24E+00	0.2666
2025	2.45E+00	0.1179
3969	9.61E-01	0.0048
7921	3.45E-01	0.1186
16129	1.20E-01	0.2191

Table 4 Example 2. Errors of standard FEM approximations on Shishkin grids for a solution with parabolic layers: even number of unknowns in the convection direction

N	$e = \ u - u_h\ _\infty$	$ \frac{\ln e}{\ln N} $
484	2.75E-03	0.9538
1024	1.76E-03	0.9153
2116	1.11E-03	0.8879
4096	7.24E-04	0.8694
8100	4.50E-04	0.8562
16384	2.68E-04	0.8475

Table 5 Example 2. Errors of standard FEM approximations on Shishkin grids for a solution with parabolic layers. Odd number of unknowns in the convection direction and the first grid size is ε

N	$e = \ u - u_h\ _\infty$	$ \frac{\ln e}{\ln N} $
441	5.59E-03	0.8520
961	2.39E-03	0.8792
2025	1.08E-03	0.8968
3969	5.38E-04	0.9085
7921	3.27E-04	0.8938
16129	1.95E-04	0.8815

Table 6 Example 2. Errors of standard FEM approximations on Shishkin grids for a solution with parabolic layers. Odd number of unknowns in the convection direction and the mid-grid size is ε

N	$e = \ u - u_h\ _\infty$	$ \frac{\ln e}{\ln N} $
441	9.29E-03	0.7684
961	3.86E-03	0.8089
2025	2.12E-03	0.8087
3969	1.37E-03	0.7959
7921	8.45E-04	0.7882
16129	5.15E-04	0.7815

oscillation of numerical solution is eliminated as well. The contour profile of the resulting smooth numerical solution is omitted since all stable and accurate solutions look the same.

Example 3: The Effect of the Perturbation of Grids

In this example, we show that the accuracy of standard finite element will decrease from N^{-1} to $N^{-1/2}$ if the grids is only quasi-uniform in the region where the solution is smooth. In contrast, the convergent rate is unchanged if only perturbing the grids inside the layer.

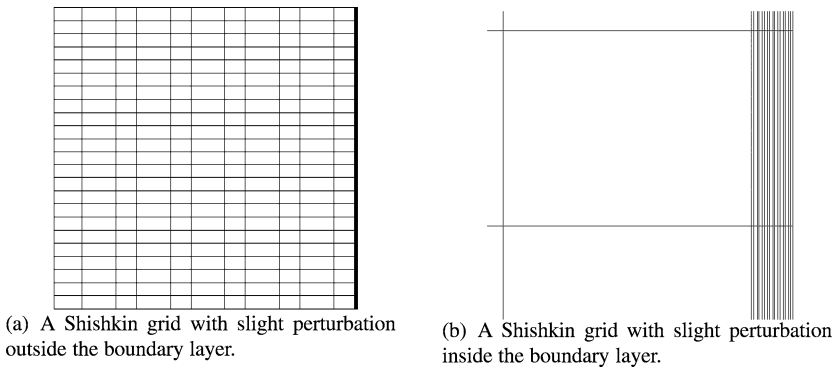


Fig. 5 Example 3. The perturbed Shishkin grids

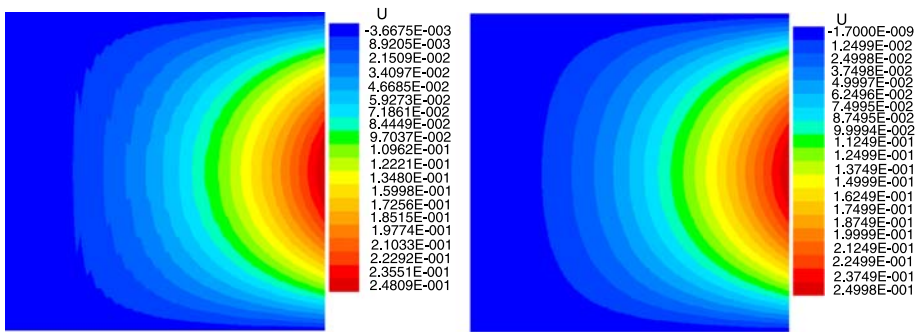


Fig. 6 (Color online) Example 3. Numerical approximations for a solution with regular boundary layer on Shishkin grids perturbed differently

Therefore the accuracy is sensitive to the symmetry of the grids and the technique of local mesh smoothing [2, 13, 16, 44] is then necessary for improving the accuracy of numerical solutions.

We pick up the stable numerical results of Example 1: the standard finite element method based on Shishkin grids for a regular boundary layer. Now in the region where the solution is smooth, we slightly move the odd grid points rightward a small amount along the convection direction $(1, 0)^T$, say $h/4$, as shown in Fig. 5(a). The numerical solution computed on such perturbed Shishkin grid is displayed in Fig. 6(a) where some wiggles are presented comparing with the smoothed solution in Fig. 6(b). The convergence rate is decreased by $1/2$ order, as shown in Table 7.

If the perturbation is conducted only inside the boundary layer while keeping the rest grids uniform, the smooth numerical solution (see Fig. 6(b)) and the optimal convergence rate (see Table 8) still hold.

We then perturb the mesh in different directions for the stabled approximation in Example 2: standard finite element based on Shishkin grids for parabolic layers and even number of unknowns in the convection direction. We perturb the grid in x -direction by moving the odd grid points in smooth region rightward $h/4$, as shown in Fig. 7(a). Table 9 shows that

Table 7 Example 3. Errors of standard FEM approximations on Shishkin grids for a solution with a regular layer. The grids are perturbed outside the boundary layer

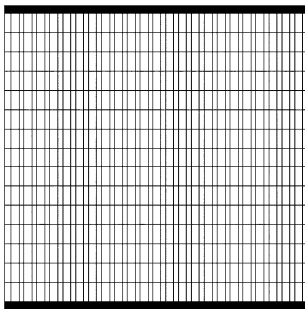
N	$e = \ u - u_h\ _\infty$	$ \frac{\ln e}{\ln N} $
484	1.54E-02	0.6756
1024	1.48E-02	0.6083
2116	9.09E-03	0.6139
4096	7.58E-03	0.5869
8100	5.08E-03	0.5871
16384	3.85E-03	0.5730

Table 8 Example 3. Errors of standard FEM approximations on Shishkin grids for a solution with a regular layer. The grids are perturbed inside the boundary layer

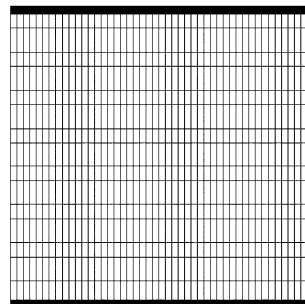
N	$e = \ u - u_h\ _\infty$	$ \frac{\ln e}{\ln N} $
484	3.23E-03	0.9277
1024	1.13E-03	0.9789
2116	1.00E-03	0.9016
4096	4.02E-04	0.9402
8100	3.42E-04	0.8867
16384	1.48E-04	0.9086

Table 9 Example 3. Errors of standard FEM approximations on Shishkin grids for a solution with parabolic layer. The grids are perturbed in x -direction

N	$e = \ u - u_h\ _\infty$	$ \frac{\ln e}{\ln N} $
484	8.88E-03	0.7642
1024	6.20E-03	0.7333
2116	4.44E-03	0.7076
4096	3.18E-03	0.6914
8100	2.29E-03	0.6757
16384	1.60E-03	0.6633



(a) A Shishkin grid with slight perturbation in x -direction.



(b) A Shishkin grid with slight perturbation in y -direction.

Fig. 7 Example 3. Shishkin grids perturbed in different directions

the convergence rate is decreased by 1/2 order because the symmetry of the grid along the convection direction (x -axis) is destroyed. This is consistent with the results in Table 7.

On the other hand, if we only perturb the odd grid points upward $h/4$ in y -direction, as shown in Fig. 7(b), the nearly optimal convergence rate is not affected; see Table 10. The reason might be that this perturbation does not change the symmetry of the grid along the convection direction.

3 Stability and Accuracy of the Streamline Diffusion Finite Element Method

In this section, we shall apply the streamline diffusion finite element method (SDFEM) to unstable approximations in Example 2 and less accurate approximations in Example 3. We shall show that SDFEM is able to recover the stability and in turn the accuracy.

To enhance the numerical stability, SDFEM or SUPG introduced in [12, 24] is to add diffusion in the convection direction. It reads as: find $u_h \in V_g^h$ such that

$$a(u_h, v_h) + \sum_{\tau \in \mathcal{T}} \delta_\tau \int_\tau (\mathbf{b} \cdot \nabla u_h + cu_h)(\mathbf{b} \cdot \nabla v_h) = f(v_h + \mathbf{b} \cdot \nabla v_h), \quad \forall v_h \in V_0^h.$$

Let the cell Péclet number be defined by

$$P_{e_\tau} := \frac{\|\mathbf{b}\|_{\infty, \tau} h_\tau}{2\varepsilon},$$

where $\|\cdot\|_{\infty, \tau}$ denotes the norm in $(L^\infty(\tau))^2$. We shall choose δ_τ suggested in [25]:

$$\delta_\tau = \begin{cases} \delta_0 \frac{h_\tau}{\|\mathbf{b}\|_{\infty, \tau}} & \text{if } P_{e_\tau} > 1 \text{ convection-dominated,} \\ \delta_1 \frac{h_\tau^2}{\varepsilon} & \text{if } P_{e_\tau} \leq 1 \text{ diffusion-dominated,} \end{cases} \tag{6}$$

Table 10 Example 3. Errors of standard FEM approximations on Shishkin grids for a solution with parabolic layer. The grids are perturbed in y -direction

N	$e = \ u - u_h\ _\infty$	$ \frac{\ln e}{\ln N} $
484	2.75E-03	0.9538
1024	1.76E-03	0.9153
2116	1.11E-03	0.8879
4096	7.24E-04	0.8694
8100	4.50E-04	0.8562
16384	2.75E-04	0.8449

Table 11 Example 4. Errors of SDFEM approximations on Shishkin grids for a solution with parabolic boundary layers. Odd number of unknowns in the convection direction

N	$e = \ u - u_h\ _\infty$	$ \frac{\ln e}{\ln N} $
441	4.09E-03	0.9030
961	2.46E-03	0.8748
2025	1.54E-03	0.8509
3969	9.50E-04	0.8398
7921	5.65E-04	0.8331
16129	3.26E-04	0.8287

Table 12 Example 4. Errors of SDFEM approximations on perturbed Shishkin grids for a solution with parabolic boundary layers

N	$e = \ u - u_h\ _\infty$	$ \frac{\ln e}{\ln N} $
484	5.17E-03	0.8516
1024	2.98E-03	0.8392
2116	1.72E-03	0.8313
4096	9.95E-04	0.8311
8100	5.56E-04	0.8327
16384	3.15E-04	0.8307

with appropriate user-chosen constants δ_0 and δ_1 .

Example 4: The Effect of SDFEM

We first recompute the unstable scheme (Shishkin grids with odd number of unknowns in the convection direction) in Example 2 using SDFEM with $\delta_0 = 0.1$ and $\delta_1 = 0$. We recovery the optimal convergent rate; see Table 11.

We then redo Example 3 on perturbed grids using SDFEM with $\delta_0 = 1.0$ and $\delta_1 = 0$. We also recovery the optimal convergent rate; see Table 12.

The above numerical experiments demonstrate that for the sake of stability, it is better to use some stabilization technique even on properly layer-adapted grids.

4 Multilevel-Homotopic-Adaptive Finite Element Methods

In this section, we shall introduce the multilevel-homotopic-adaptive finite element methods (MHAFEM). The key idea is to combine the continuation of diffusion constant and the mesh adaptation. We then present two examples to show the success of our method. One has an analytic solution that possesses regular boundary layers and the other one is a physical problem bearing with sharp interior layers.

Let us introduce the differential operator $\mathcal{L}^\varepsilon u := -\varepsilon \Delta u + \mathbf{b} \cdot \nabla u + cu$. Let \mathcal{T}_0 be an initial grid and denote by N_0 the number of elements in \mathcal{T}_0 and h_0 the mesh size of \mathcal{T}_0 . Our MHAFEM for the convection-dominated problem $\mathcal{L}^\varepsilon u := f$, which was firstly introduced in our previous work [15], can be concisely described as follows.

```

1  [uJ, TJ] = MHAFEM (T0, ε)
2  % Input: T0 initial triangulation; ε diffusion constant
3  % Output: uJ linear finite element approximation; TJ the finest mesh
4  ρ = ε0, k = 0;
5  while ρ ≥ ε
6      k = k + 1;
7      for j = 1 : max_refine
8          SOLVE: Solve Lρu = f using SDFEM on Tk to get uk;
9          ANISOTROPIC MESH ADAPTATION: Adjust the mesh to capture the
10             singularity.
11      end
12      HOMOTOPY: Reduce ρ = ρ/2. If ρ < ε, ρ = ε.
13  end
14  uJ = uk; TJ = Tk;

```

Namely, we first start our computation for large ε , and use adaptive grid technique for such diffusion-dominated elliptic problems to obtain a good initial grid. We then decrease the value of ε and apply mesh adaptation on the current grid. We continue in this way until the desired value of ε is reached. Such idea of continuously reduction of ε was also used in [32] as a continuation method for a 1-d singularly perturbed problem.

Since the singularity of layers is anisotropic, we shall apply anisotropic mesh adaptation technique developed in [13–16, 44]. These mesh adaptation techniques are developed to minimize the interpolation error in the L^p norm:

$$\|u - u_{I,T}\|_{L^p(\Omega)}, \quad 1 \leq p \leq \infty. \tag{7}$$

The key is to equidistribute the edge length under an appropriate metric related to the Hessian of the solution u . Note that finding piecewise second derivatives from piecewise linear functions leads to no approximation to Hessian matrix. Therefore special post-processing techniques need to be used to obtain reasonable Hessian matrix approximation from linear finite elements. Here we use the approach of the L^2 projection to recover piecewise linear gradient from piecewise constant gradient due to the utilization of linear finite element [4, 44].

Since the focus of this paper is on the convection-dominated problems, we refer to [14, 44] for elaborate description on the anisotropic mesh adaptation.

We list two examples below to show the success of the approach of our multilevel-homotopic-adaptive finite element method (MHAFEM).

Example 5: Approximations to a Solution with Regular Boundary Layers

We solve (2) for $\varepsilon = 10^{-4}$, $b = (2, 3)^T$ and $c = 1$. The right hand side and the boundary conditions are chosen such that the solution of (2) is

$$u(x, y) = xy^2 - y^2e^{2(x-1)/\varepsilon} - xe^{3(y-1)/\varepsilon} + e^{(2(x-1)+3(y-1))/\varepsilon}.$$

See Fig. 8 for the profile of this function. The solution u possesses typical regular boundary layers at $\{x = 1\}$ and $\{y = 1\}$.

By using MHAFEM, we obtain the convergence errors of the solutions computed on a series of anisotropic adaptive grids which are generated by the edge-based local refinement and local mesh smoothing techniques [14, 44], as shown in Table 13. The corresponding anisotropic adaptive grid for $\varepsilon = 10^{-4}$ is presented in Fig. 9.

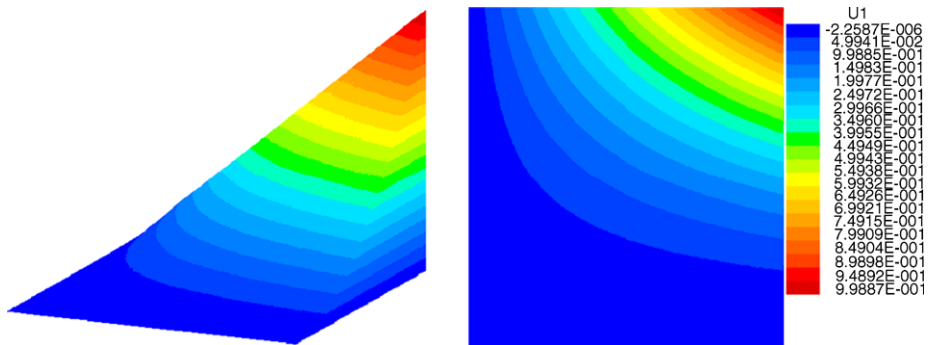
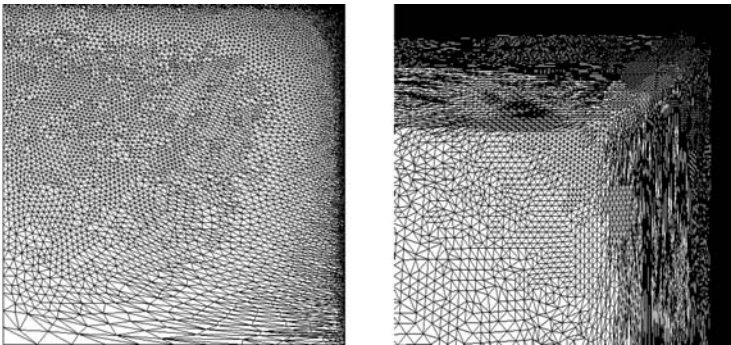


Fig. 8 (Color online) Example 5. The solution and its contour

Table 13 Example 5. Errors on anisotropic adaptive grids corresponding to decreasing ε

ε	N	$\ u - u_h\ _0$	$ \frac{\ln \ u - u_h\ _0}{\ln N} $	$\ u - u_h\ _\infty$	$ \frac{\ln \ u - u_h\ _\infty}{\ln N} $
.100D+00	1799	1.29E-04	1.19513	1.76E-03	0.84654
.500D-01	3822	1.03E-04	1.11335	1.20E-03	0.81541
.250D-01	5939	8.98E-05	1.07232	1.64E-03	0.73827
.125D-01	8637	8.37E-05	1.03577	1.93E-03	0.68943
.100D-01	11846	6.69E-05	1.02477	2.72E-03	0.62986
.500D-02	15762	6.82E-05	0.99251	2.86E-03	0.60584
.250D-02	19649	6.45E-05	0.9761	3.36E-03	0.57619
.125D-02	25531	7.15E-05	0.94076	3.32E-03	0.56258
.100D-02	30582	6.68E-05	0.93082	3.14E-03	0.5579
.500D-03	40357	7.71E-05	0.893	3.20E-03	0.54153
.250D-03	49262	9.11E-05	0.86108	2.88E-03	0.54131
.125D-03	66387	1.10E-04	0.82069	2.80E-03	0.52928
.100D-03	79104	8.38E-05	0.83233	2.68E-03	0.52518

**Fig. 9** Example 5. Anisotropic adaptive grids for $\varepsilon = 10^{-4}$

In Table 13, the convergence errors in L_2 norm are indicated in the magnitude of 10^{-5} for $\varepsilon = 10^{-4}$, and achieve nearly optimal convergence rate (second order). Meanwhile, the errors in L_∞ norm in Table 13 also reaches at least first order. Note that this problem was also tested in [25] and it was reported that, by using SDFEM and isotropic mesh adaptation, the layer still cannot be captured correctly sometimes. While using MHAFEM, we can correctly capture the layer and produce stable and accurate solution with less degree of freedoms.

Example 6: Hemker Problem

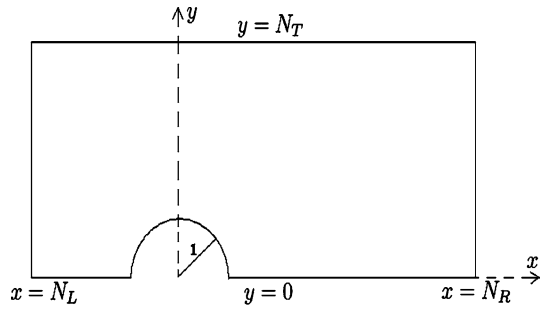
We apply our method to the Hemker problem [19]

$$-\varepsilon \Delta u + u_x = 0, \quad (8)$$

defined on the exterior of the unit disc $\Omega = \{(x, y) \in \mathbb{R}^2 | x^2 + y^2 \geq 1\}$, with boundary conditions:

$$\begin{aligned} u &= 1, & \text{if } x^2 + y^2 = 1, \\ u &\rightarrow 0, & \text{for } x^2 + y^2 \rightarrow \infty. \end{aligned} \quad (9)$$

Fig. 10 The domain of Hemker problem



The convection to right, as indicated by the convection term of (8), makes the problem symmetric with respect to a line through the origin to the right. Obviously properties of the solution are its formal smoothness, its monotonicity, and the fact that for smaller values of ϵ a sharp boundary layer appears at the upwind side of the circle, and a long “shadow region” appears at the downwind side. In the limit there is a discontinuity between the shadow (where the limit solution $u = 1$), and the ‘exposed part’ of the solution (where $u \rightarrow 0$). At the boundary of the shadow region an interior layer appears.

The original problem was defined on an unbounded domain in \mathbb{R}^2 . To numerically solve the problem by a discretization method, the infinite domain must be truncated to a finite region of interest. On the one hand the region should be large enough to contain the specific detailed of the solution and on the other hand not too large, to reduce the amount of computational work.

For its numerical solution, we truncate the domain of definition to a sufficiently large rectangle, and because of the symmetry, we only approximate the solution in half of the proposed domain. Thus, the domain we need to solve in (8) is given by a rectangle domain $\Omega = (N_L, N_R) \times (0, N_T) \setminus \{(x, y) | x^2 + y^2 \geq 1\}$, with N_L, N_R and $N_T \in \mathbb{N}$, and $0 < \epsilon \ll 1$; see Fig. 10. We specifically let $\Omega = [-4, 6] \times [0, 4] \cap \{(x, y) | x^2 + y^2 \geq 1\}$. In this way the domain can show a significant part of the solution: the boundary and interior layers, and the shadow region of the solution.

For the truncated, finite domain Ω we have to introduce artificial boundary conditions at the outer boundary. We apply the following boundary conditions:

$$\begin{aligned}
 & u(x, y) = 1 \quad \text{on } x^2 + y^2 = 1, \\
 & u(N_L, y) = 0, u_x(N_R, y) = 0 \quad \text{if } y \in [0, N_T], \\
 & u_y(x, N_T) = 0, u_y(x, 0) = 0 \quad \text{if } x \in [N_L, N_R].
 \end{aligned}
 \tag{10}$$

Note that in the case of truncated and finite domain, (8) bearing boundary conditions (10) does not own an analytic solution.

We apply our multilevel-homotopic-adaptive finite element method to solve this singular perturbation problem. To compare different solution methods, we restrict ourselves to a finite sequence of ϵ -values, viz., $\epsilon = 10^{-2}, 10^{-3}, 10^{-4}$. Here we skip those adaptive meshes and solutions in the middle process and only plot the final adaptive meshes and numerical solutions in different cases of ϵ , as shown in Figs. 11–16.

5 Conclusion and Future Work

By performing numerical tests of the standard finite element method for convection-dominated convection-diffusion-reaction problem on different layer-adapted grids, we

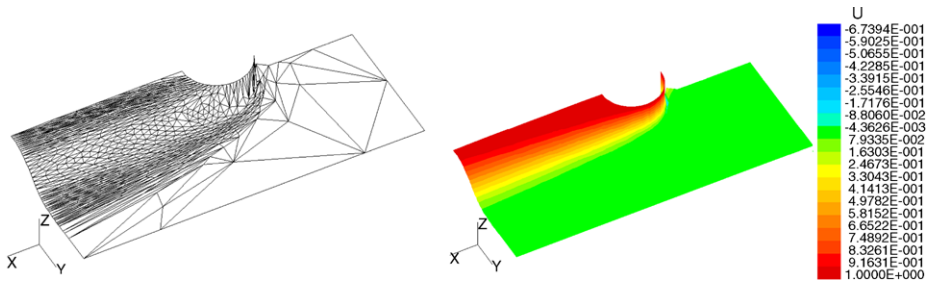


Fig. 11 (Color online) Example 6. An adaptive mesh and a solution profile for $\varepsilon = 10^{-2}$

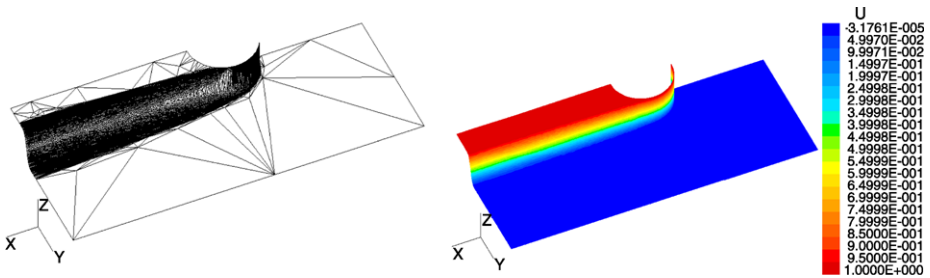


Fig. 12 (Color online) Example 6. An adaptive mesh and a solution profile for $\varepsilon = 10^{-3}$

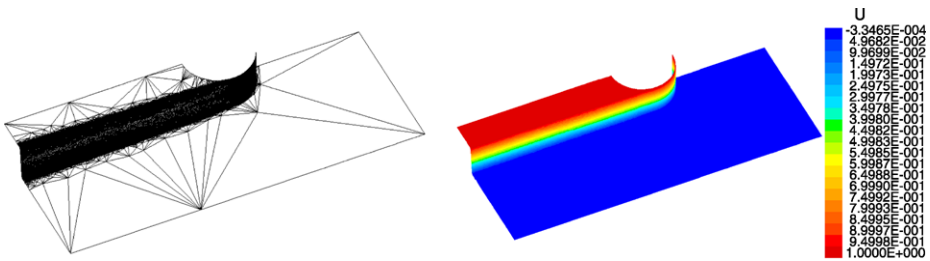


Fig. 13 (Color online) Example 6. An adaptive mesh and a solution profile for $\varepsilon = 10^{-4}$

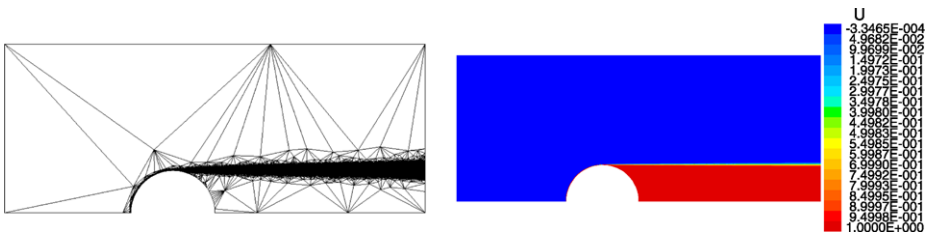


Fig. 14 (Color online) Example 6. A different visualization of an adaptive mesh and a solution profile for $\varepsilon = 10^{-4}$

demonstrate that the stabilization of a standard scheme is necessary even for the layer-adapted Shishkin grids. In particular, we show that the convergence rate is first order instead of second order in maximum norm for piecewise linear finite element when the grid is only

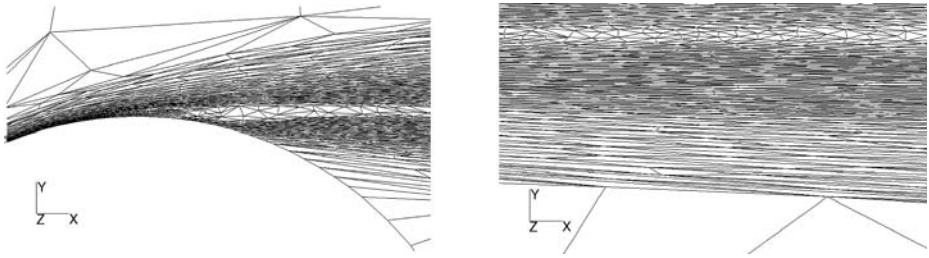


Fig. 15 (Color online) Example 6. The blow-up mesh at the tangent point and in the downstream along the tangent with $\varepsilon = 10^{-3}$

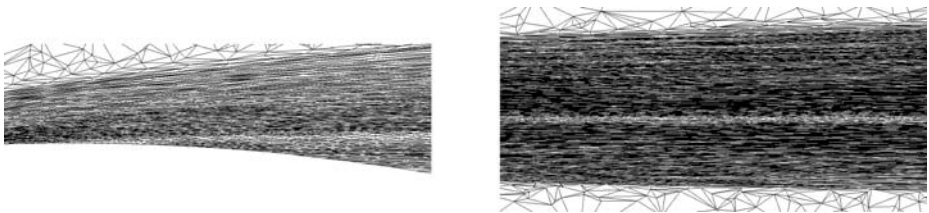


Fig. 16 Example 6. The blow-up mesh at the tangent point and in the downstream along the tangent with $\varepsilon = 10^{-4}$

quasi-uniform in the smooth part. We demonstrate that the streamline diffusion finite element method (SDFEM) on correctly adapted grids can produce both stable and accurate approximation.

For the case of solution bearing regular boundary layers, we show that Shishkin grid can increase the stability and accuracy of the standard finite element method. Whereas, for solutions with parabolic boundary layer only, the standard finite element method is unstable on Shishkin grid when the number of grid points in convection direction is odd. The stabilization and accuracy of a standard scheme are recovered by having even number of grid points or having a grid size being ε along the convection direction.

On the other hand, by perturbing Shishkin grid points outside or inside the boundary layer, we indicate that the accuracy depends crucially on the uniformity of the grids in smooth region. Generally the convergence rate is first order instead of second order in maximum norm for piecewise linear finite element when the grid is only quasi-uniform in the smooth part.

To construct a correctly adapted grid in a posteriori manner, we present an multilevel-homotopic-adaptive finite element method (MHAFEM) based on anisotropic mesh adaptation. Numerical experiments show that MHAFEM significantly reduces the number of degree of freedom and increase the accuracy in the process of achieving the desired ε . Meanwhile, the singular boundary or interior layers are accurately captured and resolved by the properly adapted grids.

We note that in our approach the anisotropic meshes generated in a posteriori manner is not as good as the Shishkin grids when a priori information, e.g., the location of the layer and the width of the layer, are known. Several mesh improvement techniques will fail when ε is as small as 10^{-8} . We could improve the robustness of the anisotropic mesh adaptation by other techniques, e.g., notably moving mesh methods [22, 29]. We do not address the issue

of the efficiency, especially the efficient solver for the linear algebraic system. Multigrid-type solvers will be deserved for further studying.

Another important ingredient is the recovery of the Hessian matrix of the solution. The accuracy of recovered derivatives of u will significantly affect the mesh adaptation. We shall test and report more robust recovery schemes in a future work.

Acknowledgements Pengtao Sun was supported by Research Development Award of University of Nevada Las Vegas 2220-320-980C. Long Chen was supported in part by NSF Grant DMS-0811272, and in part by NIH Grant P50GM76516 and R01GM75309. Jinchao Xu was supported in part by NSF Grant DMS-0609727 and Alexander H. Humboldt Foundation.

References

1. Bank, R., Bürger, J., Fichtner, W., Smith, R.: Some upwinding techniques for finite element approximations of convection diffusion equations. *Numer. Math.* **58**, 185–202 (1990)
2. Bank, R.E., Smith, R.K.: Mesh smoothing using a posteriori error estimates. *SIAM J. Numer. Anal.* **34**, 979–997 (1997)
3. Bank, R.E., Xu, J.: Asymptotically exact a posteriori error estimators, Part I: Grids with superconvergence. *SIAM J. Numer. Anal.* **41**(6), 2294–2312 (2003)
4. Bank, R.E., Xu, J.: Asymptotically exact a posteriori error estimators, Part II: General unstructured grids. *SIAM J. Numer. Anal.* **41**(6), 2313–2332 (2003)
5. Bänsch, E., Morin, P., Nochetto, R.H.: An adaptive Uzawa FEM for the Stokes problem: convergence without the inf-sup condition. *SIAM J. Numer. Anal.* **40**(4), 1207–1229 (2002)
6. Baumann, C.E., Oden, J.T.: A discontinuous hp finite element method for convection-diffusion problems. *Comput. Methods Appl. Mech. Eng.* **175**, 311–341 (1999)
7. Brezzi, F., Franca, L., Russo, A.: Further considerations on residual free bubbles for advection-diffusive equations. *Comput. Methods Appl. Mech. Eng.* **166**, 25–33 (1998)
8. Brezzi, F., Franca, L.P., Hughes, T.J.R., Russo, A.: $b = \int g$. *Comput. Methods Appl. Mech. Eng.* **145**, 329–339 (1997)
9. Brezzi, F., Hughes, T.J.R., Marini, L.D., Russo, A., Süli, E.: A priori error analysis of residual-free bubbles for advection-diffusion problems. *SIAM J. Numer. Anal.* **36**(4), 1933–1948 (1999)
10. Brezzi, F., Marini, D., Süli, E.: Residual-free bubbles for advection-diffusion problems: the general error analysis. *Numer. Math.* **85**, 31–47 (2000)
11. Brezzi, F., Marini, L.D., Pietra, P.: Two-dimensional exponential fitting and applications to drift-diffusion models. *SIAM J. Numer. Anal.* **26**(6), 1342–1355 (1989)
12. Brooks, A., Hughes, T.: Streamline upwind/Petrov-Galerkin formulations for convection dominated flows with particular emphasis on the incompressible Navier-Stokes equations. *Comput. Meth. Appl. Mech. Eng.* **32**, 199–259 (1982)
13. Chen, L.: Mesh smoothing schemes based on optimal Delaunay triangulations. In: 13th International Meshing Roundtable, Williamsburg, VA, 2004, pp. 109–120. Sandia National Laboratories, Albuquerque (2004)
14. Chen, L.: Robust and accurate algorithms for solving anisotropic singularities. PhD thesis, Department of Mathematics, The Pennsylvania State University (2005)
15. Chen, L., Sun, P., Xu, J.: Multilevel homotopic adaptive finite element methods for convection dominated problems. In: The Proceedings for 15th Conferences for Domain Decomposition Methods. Lecture Notes in Computational Science and Engineering, vol. 40, pp. 459–468. Springer, Berlin (2004)
16. Chen, L., Sun, P., Xu, J.: Optimal anisotropic simplicial meshes for minimizing interpolation errors in L^p -norm. *Math. Comput.* **76**(257), 179–204 (2007)
17. Chen, L., Xu, J.: Stability and accuracy of adapted finite element methods for singularly perturbed problems. *Numer. Math.* **109**(2), 167–191 (2008)
18. Heinrich, J.C., Huyakorn, P.S., Zienkiewicz, O.C., Mitchell, A.R.: An ‘upwind’ finite element scheme for two-dimensional convective transport equation. *Int. J. Numer. Methods Eng.* **11**, 131–143 (1977)
19. Hemker, P.W.: A singularly perturbed model problem for numerical computation. *J. Comput. Appl. Math.* **76**(1–2), 277–285 (1996)
20. Holmes, M.H.: Introduction to Perturbation Methods. Texts in Applied Mathematics, vol. 20. Springer, New York (1995)
21. Houston, P., Schwab, C., Süli, E.: Discontinuous hp -finite element methods for advection-diffusion-reaction problems. *SIAM J. Numer. Anal.* **39**(6), 2133–2163 (2002)

22. Huang, W.: Mathematical principles of anisotropic mesh adaptation. *Commun. Comput. Phys.* **1**, 276–310 (2006)
23. Huang, W., Sun, W.: Variational mesh adaptation II: error estimates and monitor functions. *J. Comput. Phys.* **184**, 619–648 (2003)
24. Hughes, T.J.R., Brooks, A.: A multidimensional upwind scheme with no crosswind diffusion. In: Hughes, T.J.R. (ed.) *Finite Element Methods for Convection Dominated Flows*. AMD, vol. 34, pp. 19–35. ASME, New York (1979)
25. John, V.: A numerical study of a posteriori error estimators for convection-diffusion equations. *Comput. Methods Appl. Mech. Eng.* **190**(5–7), 757–781 (2000)
26. John, V., Knobloch, P.: On spurious oscillations at layers diminishing (SOLD) methods for convection-diffusion equations: part I—a review. *Comput. Methods Appl. Mech. Eng.* **196**(17–20), 2197–2215 (2007)
27. John, V., Knobloch, P.: On spurious oscillations at layers diminishing (SOLD) methods for convection-diffusion equations: part II—analysis for P1 and Q1 finite elements. *Comput. Methods Appl. Mech. Eng.* **197**, 1997–2014 (2008)
28. Kang, T., Yu, D.: Some a posteriori error estimates of the finite-difference streamline-diffusion method for convection-dominated diffusion equations. *Adv. Comput. Math.* **15**, 193–218 (2001)
29. Li, R., Tang, T., Zhang, P.: Moving mesh methods in multiple dimensions based on harmonic maps. *J. Comput. Phys.* **170**(2), 562–588 (2001)
30. Li, R., Tang, T., Zhang, P.: A moving mesh finite element algorithm for singular problems in two and three space dimensions. *J. Comput. Phys.* **177**(2), 365–393 (2002)
31. Linß, T.: Analysis of a Galerkin finite element method on a Bakhvalov-Shishkin mesh for a linear convection-diffusion problem. *IMA J. Numer. Anal.* **20**, 621–632 (2000)
32. Linß, T.: The necessity of Shishkin-decompositions. *Appl. Math. Lett.* **14**, 891–896 (2001)
33. Linß, T.: Layer-adapted meshes for convection-diffusion problems. *Comput. Methods Appl. Mech. Eng.* **192**, 1061–1105 (2003)
34. Linß, T., Stynes, M.: Numerical methods on Shishkin meshes for linear convection-diffusion problems. *Comput. Methods Appl. Mech. Eng.* **190**(28), 3527–3542 (2001)
35. Linß, T., Stynes, M.: The SDFEM on Shishkin meshes for linear convection-diffusion problems. *Numer. Math.* **87**, 457–484 (2001)
36. Miller, J.J.H., O’Riordan, E., Shishkin, G.I.: On piecewise-uniform meshes for upwind- and central-difference operators for solving singularly perturbed problems. *IMA J. Numer. Anal.* **15**, 89–99 (1995)
37. Miller, J.J.H., O’Riordan, E., Shishkin, G.I.: *Fitted Numerical Methods for Singular Perturbation Problems*. World Scientific, Singapore (1996)
38. Morton, K.W.: *Numerical Solution of Convection-Diffusion Problems*. Applied Mathematics and Mathematical Computation, vol. 12. Chapman & Hall, London (1996)
39. Nooyen, R.R.P.V.: A Petrov-Galerkin mixed finite element method with exponential fitting. *Numer. Methods Partial Differ. Equ.* **11**(5), 501–524 (1995)
40. Roos, H.G., Stynes, M., Tobiska, L.: *Numerical Methods for Singularly Perturbed Differential Equations*. Springer Series in Computational Mathematics, vol. 24. Springer, Berlin (1996)
41. Roos, H.G.R.G.: A note on the conditioning of upwind schemes on Shishkin meshes. *IMA J. Numer. Anal.* **16**, 529 (1996)
42. Shishkin, G.I.: Grid approximation of singularly perturbed elliptic and parabolic equations. PhD thesis, Second doctoral thesis, Keldysh Institute, Moscow (1990) (in Russian)
43. Stynes, M.: Steady-state convection-diffusion problems. *Acta Numer.* **14**, 445–508 (2005)
44. Sun, P., Russell, R.D., Xu, J.: A new adaptive local mesh refinement algorithm and its application on fourth order thin film flow problem. *J. Comput. Phys.* **224**(2), 1021–1048 (2007)
45. Tobiska, L.: Analysis of a new stabilized higher order finite element method for advection-diffusion equations. *Comput. Methods Appl. Mech. Eng.* **196**, 538–550 (2006)
46. Xu, J., Zikatanov, L.: A monotone finite element scheme for convection diffusion equations. *Math. Comput.* **68**, 1429–1446 (1999)
47. Zhang, Z., Tang, T.: An adaptive mesh redistribution algorithm for convection-dominated problems. *Commun. Pure Appl. Anal.* **1**(3), 341–357 (2002)
48. Zhang, Z.M.: Finite element superconvergence on Shishkin mesh for 2-D convection-diffusion problems. *Math. Comput.* **72**(243), 1147–1177 (2003)